Contents lists available at Science-Gate

International Journal of Advanced and Applied Sciences

Journal homepage: http://www.science-gate.com/IJAAS.html

Adsorption of phosphate from synthetic solution onto the limestone in a plug-flow column

Mohd Hairul Khamidun [1, *], Mohamad Ali Fulazzaky [2]

[1]*Faculty of Civil and Environmental Engineering, University Tun Hussein Onn Malaysia, Batu Pahat, Johor, Malaysia*
[2]*Institute of Environmental and Water Resources Management, Water Research Alliance, University Technology Malaysia Skudai, Johor Bahru, Johor, Malaysia*

ARTICLE INFO

Article history:
Received 27 December 2015
Received in revised form
15 January 2016
Accepted 15 January 2016

Keywords:
Adsorption
Limestone
Mass transfer factor models
Phosphate
Plug-flow column

ABSTRACT

The removal of phosphate (PO_4^{3-}) from a synthetic solution by adsorbing onto the limestone was performed in a plug-flow column reactor (PFCR) treatment process. The experiments were conducted using three different flow rates of 1.56, 2.80 and 3.91 mL min^{-1}. Thomas and Yoon-Nelson models were applied to experimental data to understand adsorption behaviour, while, the mass transfer factor (MTF) models were used to investigate the effect of flow rate on the resistance of mass transfer of PO_4^{3-} onto the limestone. The results show that the saturation time increased with decrease in flow rate. The dynamic adsorption behaviour was satisfactory described by Thomas and Yoon-Nelson models. The MTF models verified that the resistance of mass transfer could be dependent on porous diffusion until the percentage of outflow reaches 72% and 86% for flow rates of 1.56, 2.80 mL min^{-1}, respectively. Even though, film mass transfer can play a minor role in controlling the movement of PO_4^{3-} from the bulk water to film zone of limestone. The results of the $[k_La]_g$ $[k_La]_f$ and $[k_La]_d$ coefficients obtained from application of MTF models could be applied to understand the mechanism of mass transfer mechanism of mass transfer of PO_4^{3-} across liquid-solid interfaces.

1. Introduction

Phosphorus is essential for deoxyribonucleic acid, ribonucleic acid, and energy transfer of organisms (Conley et al., 2009). Nevertheless, the enrichment of phosphorus in waters can influence the rapid growth of phytoplankton and macrophytes that can cause eutrophication. Nowadays, various techniques of treatment can be used to remove phosphorus from waters such as biological phosphorus removal, air stripping, chemical precipitation and adsorption. However, the biological process to treat wastewater requires high investment and annual operating costs (Guieysse and Norvill, 2014). The disadvantages for using the chemical method are the high chemical costs, additional chemicals will be created, and increasing sludge volume (Al-Shannag et al., 2015). Among all water treatment techniques, the adsorption process is one of the purification technologies and can be utilized to remove phosphorus from the water. This method requires simple operation and design, and draws up a small amount of sludge. The adsorption technique widely used to remove phosphorus from the water. For instance, this method requires a simple operation and design as well as produces a small amount of sludge. The adsorption of phosphorus from waters onto natural materials such as limestone, zeolite, goethite, iron ore, laterite and sand has been reported by a number of researchers (Hussain et al., 2011; Zeng et al., 2004). The potential of the use of limestone to adsorb PO43- from waters has been investigated by many researchers (Hussain et al., 2011; Karczmarczyk and Bus, 2014; Mateus et al., 2012; Price et al., 2010).

The adsorption of PO43- from synthetic solution by limestone as reported by Karczmarczyk and Bus (2014) can achieve approximately 11.12 mg g-1 of the adsorption capacity. The adsorption of PO43- onto a mixture of GAC and limestone from domestic wastewater was performed with a concentration range of 9 - 25 mg L-1; the optimum removal of PO43- with 93% efficiency and that of NH4+ with 58% efficiency of using the mixture ratio of limestone/GAC of 25/15 has been verified (Hussain et al., 2011). The use of fragmented Moleanos limestone as substrate in constructed wetlands can be used to remove PO43- from surface water, resulted in 61% ± 7 of the removal efficiency (Mateus et al., 2012). Even if the limestone

* Corresponding Author.
Email Address: mhairulk@gmail.com

promising adsorbent for removing PO43- from aqueous solution, the use of MTF models for scrutinising the resistance of mass transfer still not fully understand. The objectives of this study are to investigate the dynamic adsorption behaviour of PO43- onto limestone by using Thomas and Yoon-Nelson models; to use the MTF models to determine the variations of [kLa]g [kLa]f and [kLa]d factor independently for the adsorptions of PO43-onto limestone at different flow rates; and to analyse the surface functional groups to confirm the adsorption of PO43- ion onto limestone.

2. Materials and methods

2.1. Preparation of limestone and synthetic solution

The limestone was obtained from a cement manufacturing plant in Negeri Sembilan, Malaysia. The limestone was crushed and passed through a 2.13 mm mesh sieve and retained on 1.18 mm mesh sieve. Approximately 5 kg of the limestone was washed with distilled water and dried at 103oC for 24 h in an oven. The dried limestone used as adsorbent for the adsorption of PO43- from synthetic solution in PFCR. Fourier transform infrared (FTIR) analysis was performed on KBr pellets using a Spectrum One FT-IR Spectrometer (Perkin Elmer Instruments, USA) in the wavenumber range between 600 and 4000 cm-1. The FTIR spectral characteristics can be useful for investigation of the surface functional groups at the surface of the limestone.

Synthetic solution with concentration of 100 mg L-1 of PO43- was prepared by dissolving a 0.4394 g of KH2PO4 (analytic grade) into 1 L of deionised water in a volumetric flask. The synthetic solution was successively diluted with deionised water to obtain the desired test concentration of solute. The pH of the synthetic solutions was set up at 6.5 for all the plug-flow column experiments.

2.2. Plug-flow column reactor

A schematic diagram for the laboratory scale plug-flow column reactor is shown in Fig. 1. The plug-flow columns were made of acrylic tubes 2.1 cm internal diameter and 70 cm in height. The bed depth used in the experiments was 68 cm. In a typical experiment the known concentration of PO43- in synthetic solution was pumped using a Masterflex peristaltic pump at flow rates of 1.56, 2.80 and 3.91 mL min-1 to fill the plug-flow column height. The concentration of PO43- at inlet of the PFCR (storage tank), outlet of the PFCR treatment system were intermittently collected at defined time intervals and analysed based on Amino acid method using HACH DR 6000 UV–Vis Spectrophotometer.

The total adsorbed PO43- quantity in the limestone filled bed of PFCR for a given feed concentration and flow rate can be calculated by the following equation:

$$q = (Co - Cs)\, V / m \quad (1)$$

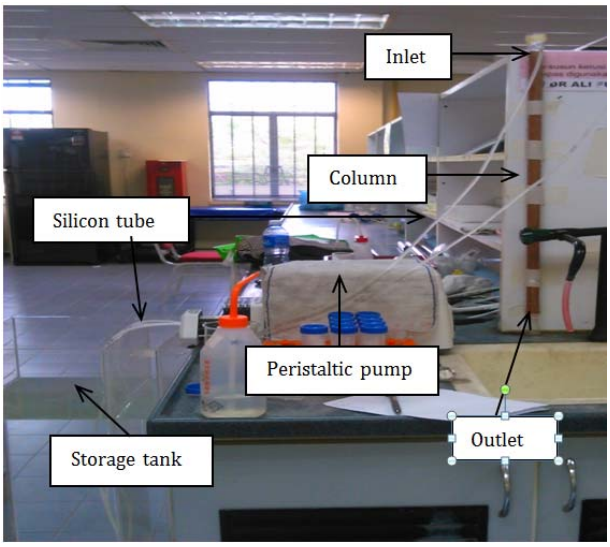

Fig. 1: The experimental setup

where, q is the cumulative quantity of PO43- to adsorb onto the limestone (mg g-1), Co is the concentration of PO43- to entry into the column (mg L-1), Cs is the concentration of PO43- to depart from the column (mg L-1), V is the effective volume of the treated water (L) and m is the amount of adsorbent in the column (g).

3. Empirical adsorption models

3.1. Thomas model

Thomas model (Thomas, 1943) is based upon the assumptions that: (1) there is negligible axial and radial dispersion in the fixed bed column; (2) the adsorption is described by a pseudo second-order reaction; (3) the column of void fraction is constant; (4) the physical properties of the adsorbent (solid-phase) and the fluid phase during the adsorption process are approximately similar; (5) the adsorption process has the isothermal and isobaric conditions; (6) the resistances of porous diffusion and film mass transfer are negligible (Tefera et al., 2014). The linearised form of this model can be described by the following:

$$ln(Co/Cs - 1) = ((kT \times qo \times m / Q) - 1) \times kT \times Co \times t \quad (2)$$

where Cs is the concentration of the PO43- to depart from the column (in mg L-1), Co is the concentration of the solute to enter into the column (in mg L-1), kT is the kinetic coefficient or the Thomas rate constant (in L h-1 mg-1), qo is the equilibrium solute uptake per gram of the adsorbent bed (in mg g-1), m is the amount of limestone in the column (g) Q is the volumetric flow rate (in L h-1) and t is the accumulation time or the service time (in h).

The kinetic coefficient kT and the equilibrium solute uptake per gram of the adsorbent bed (qo)

can be determined from a plot of ln [(Co/Cs) − 1] versus t at a given flow rate, which gives a straight line intercept at kT × qo × m/Q and kT × Co as slope.

3.2. Yoon-Nelson model

The Yoon-Nelson models originally developed by Yoon and Nelson, (1984) can be used to assess the performance of PFCR. This model is based on the assumption that the rate of decrease in the probability of adsorption of adsorbate molecule is proportional to the probability of the adsorbate adsorption and the adsorbate breakthrough on the adsorbent. The linearised form of the model is given as (Woumfo et al., 2015):

$$ln(Cs/(Co - Cs)) = (kYN \times t) - (\tau \times kYN) \quad (3)$$

where Cs is the concentration of the PO43- to depart from the column (in mg L-1), Co is the concentration of the solute to enter into the column (in mg L-1), kYN is the Yoon–Nelson rate constant (in h-1), t is the accumulation time or the service time (in h) and τ is the time required for 50% adsorbate breakthrough (in h).

The Yoon–Nelson rate constant kYN and the time required for 50% adsorbate breakthrough τ can be determined from a plot of ln [(Cs/ Co - Cs)] versus t at a given flow rate, which gives a straight line intercept at τ × kYN and kYN as slope.

Mass transfer factor models

MTF models (Fulazzaky et al., 2013) were used for understanding the mechanisms of mass transfer for adsorption of PO43- from aqueous solution onto porous material. The MTF models are expressed in equation (4):

$$ln(Co/Cs) = [kLa]g \times e - \beta \times ln(q) \times t \quad (4)$$

where Cs is the concentration of the PO43- to depart from the column (in mg L-1), Co is the concentration of PO43- to enter into the column (in mg L-1), [kLa]g is the global mass transfer factor (in min-1), β is the absorbent–adsorbent affinity parameter (g h mg-1); q is the cumulative quantity of the solute to adsorb onto limestone (in mg g-1); and t is the accumulation time (min).

The mathematical deduction of equation (4) can be simplified as:

$$ln(q) = (1/\beta) \times ln(t) + B \quad (5)$$

with

$$B = (ln([kLa]g) - ln\{ln(Co/Cs)\})/\beta \quad (6)$$

where B is the potential mass transfer index relating to driving force of the mass transfer (in mg g-1)

The value of [kLa]g can be determined using equation (6) since the index B and the parameter β has been verified on a straight line of a plot of ln(q) versus ln(t) . Equation (7) permits the computation of [kLa]f, and equation (8) can be used to determine [kLa]d.

$$[kLa]f = [kLa]g \times e - \beta \times ln(q) \quad (7)$$

$$[kLa]d = [kLa]g - [kLa]f \quad (8)$$

where [kLa]f is the film mass transfer factor (in min-1); and [kLa]d is the porous diffusion factor (in min-1).

4. Results and discussions

4.1. Plug-flow column dynamic studies

The effect of flow rate on performance of the plug-flow column was investigated at flow rates of 1.56, 2.80 and 3.91 mL min-1 at pH 6.5 and initial PO43- concentration of 12.7 mg/L. Fig. 2 shows the breakthrough curves for the adsorption of PO43- onto the limestone from synthetic solution. As shown in Fig. 2, the saturation time increased with decreasing flow rate due to the fact that the slow flow rate can lead to increase contact time between PO43- ions and active sites on the surface of limestone, resulted in increased saturation time. For instance, an increase flow rate from 1.56 to 2.80 and to 3.90 mL min-1 decreased the saturation time (Cs/Co ≈ 0.95) from 192 to 46 to 8 min, respectively.

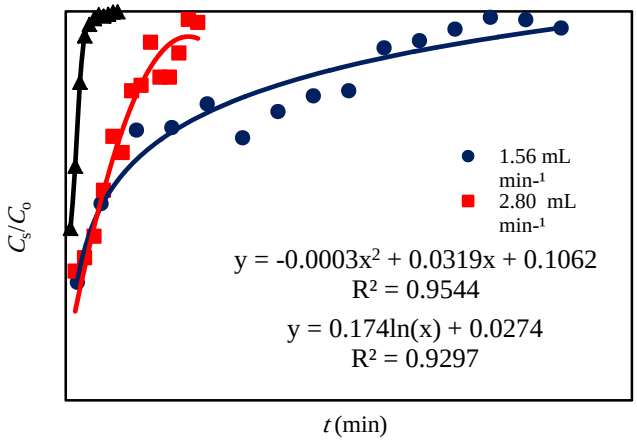

Fig. 2: Breakthrough curves for the adsorption of PO43- onto limestone from synthetic solution at different flow rates

4.2. Application of Thomas model

The use of Thomas models could be useful to scrutinise behaviour for the adsorption of PO43- onto limestone and to determine the plug-flow column performance. A plot of ln[(Co/Cs) – 1] versus t gives us a straight line, with kT is slope and qo is interception of the vertical-axis. The values for the parameters kT and qo are presented in Table 1. Correlation for the curves of plotting ln[(Co/Cs) – 1] versus t is good (R2 > 0.93; see Table. 3), meaning that the values of kT and qo can be used to describe the adsorption behaviour. The increase in kT value might indicates the decreased resistance of mass transfer (Meng et al., 2013) while the increase in qo value might indicates the additional of driving force for the adsorption of PO43- onto limestone (Guo et al., 2013), as the flow rate increases. Even though the use of Thomas models could be used to describe the adsorption behaviour, such the empirical models are

still not applicable in evaluating the mechanisms of mass transfer from the bulk water to acceptor sites at the surface of limestone for the adsorption of one or more solutes present in water.

Table 1: Analysis of the use Thomas models for the adsorption of PO43- onto limestone

h (cm)	Q (mL min-1)	R2	kT (L min-1mg-1)	qo (mg g-1)
70	1.56	0.93	0.0018	1.61
70	2.80	0.94	0.0067	1.39
70	3.91	0.96	0.0273	0.23

4.3. Application of Yoon-Nelson model

The Yoon-Nelson models were used to analyse the experimental data in order to understand the behaviour of the adsorption of PO43- from synthetic solution onto limestone in PFCR. Correlation for the parameters kYN and τ in equation (3) is good, indicating with R2 greater than 0.91 (see Table 2). This means that the Yoon-Nelson can be used to describe the breakthrough behaviour of - onto limestone because of the models have been verified as good empirical equations applied to a PFCR. The fact (see Table 2) is that the value of kYN increases from 0.0234 to 0.0847 and to 0.3467 L min-1 mg-1 with increasing of the flow rate from 1.56 to 2.80 and to 3.91 mL min-1, respectively. Such a phenomenon would be related to the transport of PO43- ions from bulk water to acceptor sites at the surface of limestone, which probably increases with increasing the rate of water flow through the plug column (Yang et al., 2015). The decrease in τ value may be due to the fact that the increase in flow rate can lead to having short contact time between the solute and adsorbent resulted in comparatively lower the time required for 50% PO43- breakthrough at higher flow rate (Nguyen et al. 2015).

Table 2: Analysis of the use Yoon-Nelson models for the adsorption of PO43- onto limestone

h (cm)	Q (mL min-1)	kYN (min-1)	τ × kYN	τ (min)	R2
70	1.56	0.0234	0.667	28.5	0.93
70	2.80	0.0847	1.160	13.7	0.92
70	3.91	0.3467	0.566	1.6	0.91

4.4. Application of mass transfer factor models

A plot (Fig. 3) of ln(q) versus ln(t) gives us a straight line, intercept at B and β-1 is slope. Correlation for all the parameters in equation (5) is very good (R2 > 0.95; except for flow rate of 3.91 mL min-1 in which R2 = 0.78, see Fig. 3), meaning that both the index B and parameter β could be useful for scrutinising the mass transfer potential and the affinity of adsorbate–adsorbent for the adsorption of PO43- onto limestone from synthetic solution. However, correlation for parameters B and β is not good for flow rate of 3.91 mL min-1 due to the unavailability of sufficient retention time, and the limited diffusivity of the PO43- ions into the active sites or pores of the limestone (Shanmugaprakash et al., 2014). Thus, the variations of [kLa]g [kLa]f and [kLa]d can be evaluated only for flow rates of 1.56 and 2.80 mL min-1.

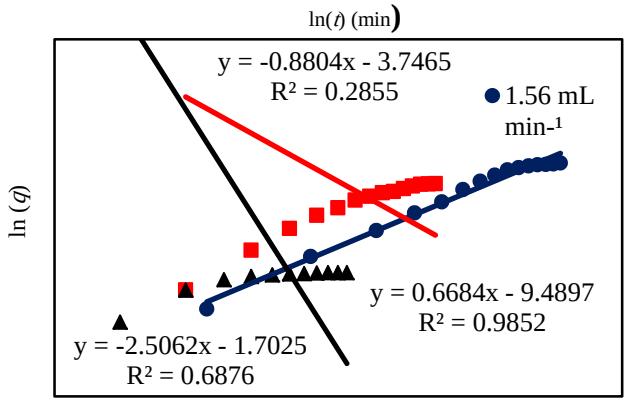

Fig. 3: Linear regression analyses for ln(q) versus ln(t) for the adsorption of PO43- onto limestone

The experimental data validation was found that the value of β increases from 1.496 and to 1.536 g min mg-1 and the value of B also increase from -9.489 and to -8.894 mg g-1 with increasing of the flow rate from 1.56 and to 2.80 mL min-1, respectively. The value of β increases with increasing of the flow rate could be due to the high flow rate would decrease resistance of mass transfer in bulk of water (Sheshdeh et al., 2014). The adsorption of PO43- onto limestone is easily affected by both van der Waals force and chemical interaction and could have a strong affinity of the absorbate–adsorbent (Fulazzaky, 2012; Fulazzaky, 2011). The increases in B value could be due to a high PO43- concentration in the stagnant film on the water side of the interface, affecting the value of driving force reduces because of the difference in PO43- concentration between the bulk water and film zone lowers (Fulazzaky et al., 2014; Khamidun et al., 2014).

Mass Transfer Resistance

Using equation (6) permits us to determine the variations of [kLa]g pursuant to the percentage of outflow if the parameters B and β were verified. Fig. 4 shows the variations of [kLa]g decreased progressively from a high to low mass transfer potential with increasing of the percentage of outflow. The variation of [kLa]g value for a flow rate of 2.80 mL min-1 is quite high when comparing to flow rate of 1.56 mL min-1. This could be due to a high rate of water flow passing through a packed-bed column can cause a rapid movement of PO43- from the bulk water to acceptor sites at the surface of limestone.

Based on the curves in Fig. 5 (a and b), the variations of [kLa]f and [kLa]d pursuant to the percentage of outflow can be used to determine the resistance of mass transfer for the adsorption of PO43- onto limestone from synthetic solution, which would be dependent on either film mass transfer or porous diffusion. Evidence shows that the variations of [kLa]f rapidly decrease, counterbalanced by the variations of [kLa]d rapidly increase, when the

percentages of outflow are still less than 50 and 42% for the experimental runs with the flow rates of 1.56 and 2.80 mL min-1, respectively. As a conclusion, the application of the mass transfer factor models can determine that the resistance of mass transfer for the adsorption of PO43- onto limestone from synthetic solution could be obviously dependent on porous diffusion.

4.5. FTIR analysis

Fig. 6 (a and b) depicts the difference in FTIR spectra of the limestone before and after adsorption of the PO43- ions. The spectra peaks at 2.325; 1,163; 877 and 750 cm-1 for raw limestone can be indicated to presence of calcite (Sdiri et al., 2010). Thus, evidence show that the limestone is mainly composed of calcium in the form of calcite as identified by its major peaks (Gunasekaran et al., 2006). The peaks occurring at 3,647 and 3,671 of before and after adsorption of PO43- are corresponded the absorbance of the outer hydroxyl ions (Van Oers et al., 2014).

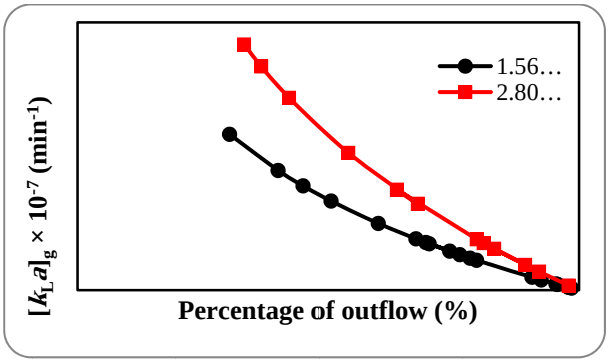

Fig. 4: Variations of [kLa]g pursuant to the percentage of outflow for different flow rates

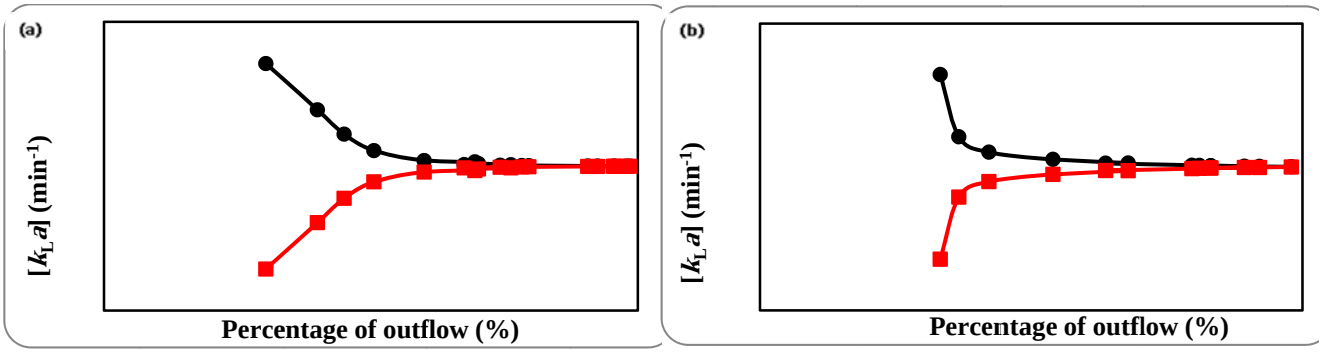

Fig. 5: Variations of: [kLa]f (black) and [kLa]d (red) pursuant to the percentage of outflow for flow rates of (a) 1.56 mL min-1 and (b) 2.80 mL min-1

The spectra of limestone after adsorption of PO43- shows the different frequency of 25 cm-1 (1,425 – 1,400 cm-1) is due to triply degenerate asymmetric stretching vibration mode of the carbonated groups, may be explained by the fact that indicate the presence of CO32- substituting for PO43- in the limestone, confer their ability to increase adsorbate-adsorbent affinity (Luickx et al., 2015). The peak at 1326 cm-1 (assigned as C-O bond) disappear after adsorption of PO43- due to the PO43- was incorporated into the structure of limestone during the adsorption process by substitution of carbonate ions by PO43- (Loganathan et al., 2013). The peaks shifted from 877 to 872 cm-1 and 750 to 711 cm-1 can be assigned as the out-of-plane and in-plane deformation modes of carbonate, respectively (Flores-Cano et al., 2013), which suggested that the formation calcium phosphate (CaHPO4; Ca(PO4)2) when limestone in contact with PO43-.

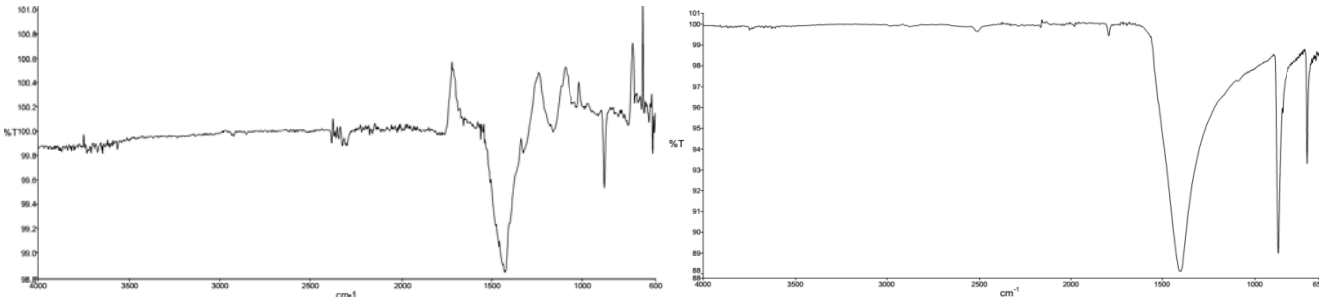

a b

Fig. 6: FTIR spectra of the limestone (a) before and (b) after the adsorption of PO43- ions

5. Conclusion

The adsorption of PO43- in PFCR using limestone is an effective and feasible process. The experimental data obtained was experimentally and theoretically studied. The saturation time was increased with decreasing flow rate. The experimental data obtained from the adsorption process in plug-flow column at bed depths of 2, 4, 6, 9, 12 and 15 were successfully correlated with the Thomas (R2 > 0.93),

Yoon-Nelson (R2 > 0.91) and MTF models (R2 > 0.95). The qo of PO43- as high as 1.61, 1.39 and 0.23 mg g-1 were verified by using Thomas model for flow rate of 1.56, 2.80 and 3.91 mL min-1, respectively. The variation of [kLa]g, [kLa]f and [kLa]d were affected by flow rate. The resistance of mass transfer for the adsorptions of PO43- onto limestone in synthetic solution from a PFCR is dependent on the porous diffusion. The methodology described and carried out here can be easily used to understand the mechanisms of global, external and internal mass transfer for the adsorption of PO43- onto limestone and to facilitate performance the PFCR effectiveness in removal pollutants from water.

Acknowledgement

We thank the Universiti Teknologi Malaysia (UTM) for financial support of Research University Grant (Vot. No. 07H01).

References

Al-Shannag M, Al-Qodah Z, Bani-Melhem K, Qtaishat MR and Alkasrawi M (2015). Heavy metal ions removal from metal plating wastewater using electrocoagulation: Kinetic study and process performance. Chemical Engineering Journal, 260: 749-756.

Conley DJ, Paerl HW, Howarth RW, Boesch DF, Seitzinger SP, Havens KE and Likens GE (2009). Controlling eutrophication: nitrogen and phosphorus. Science, 323(5917): 1014-1015.

Flores-Cano JV, Leyva-Ramos R, Mendoza-Barron J, Guerrero-Coronado RM, Aragón-Piña A and Labrada-Delgado GJ (2013). Sorption mechanism of Cd (II) from water solution onto chicken eggshell. Applied Surface Science, 276: 682-690.

Fulazzaky MA, Khamidun MH, Din MFM and Yusoff ARM (2014). Adsorption of phosphate from domestic wastewater treatment plant effluent onto the laterites in a hydrodynamic column. Chemical Engineering Journal, 258: 10-17.

Fulazzaky MA, Khamidun MH and Omar R (2013). Understanding of mass transfer resistance for the adsorption of solute onto porous material from the modified mass transfer factor models. Chemical Engineering Journal, 228: 1023-1029.

Fulazzaky MA (2012). Analysis of global and sequential mass transfers for the adsorption of atrazine and simazine onto granular activated carbons from a hydrodynamic column. Analytical Methods, 4(8): 2396-2403.

Fulazzaky MA (2011). Determining the resistance of mass transfer for adsorption of the surfactants onto granular activated carbons from hydrodynamic column. Chemical Engineering Journal, 166(3): 832-840.

Guieysse B and Norvill ZN (2014). Sequential chemical–biological processes for the treatment of industrial wastewaters: Review of recent progresses and critical assessment. Journal of Hazardous Materials, 267: 142-152.

Gunasekaran S, Anbalagan G and Pandi S (2006). Raman and infrared spectra of carbonates of calcite structure. Journal of Raman Spectroscopy, 37(9): 892-899.

Guo M, Li M, Dai Y, Shen W, Peng J, Zhu C and He R (2013). Exploring the role of varied-length spacers in charge transfer: a theoretical investigation on pyrimidine-bridged porphyrin dyes. RSC Advances, 3(38): 17515-17526.

Hussain S, Aziz HA, Isa MH, Ahmad A, Van Leeuwen J, Zou L and Umar M (2011). Orthophosphate removal from domestic wastewater using limestone and granular activated carbon. Desalination, 271(1): 265-272.

Karczmarczyk A and Bus A (2014). Testing of reactive materials for phosphorus removal from water and wastewater–comparative study. Annals of Warsaw University of Life Sciences-SGGW. Land Reclamation, 46(1): 57-67.

Khamidun MH, Fulazzaky MA, Din MFM and Yusoff ARM (2013). Resistance of mass transfer, kinetic and isotherm study of ammonium removal by using a Hybrid Plug-Flow Column Reactor (HPFCR). In: 2nd International Conference on Frontier of Energy and Environment Engineering (ICFEEE 2013), 28 – 29 November 2013, XiaMen, China.

Loganathan P, Vigneswaran S, Kandasamy J and Bolan NS (2014). Removal and recovery of phosphate from water using sorption. Critical Reviews in Environmental Science and Technology, 44(8): 847-907.

Luickx N, Van Den Vreken N, Segaert J, Declercq H, Cornelissen M and Verbeeck R (2015). Optimization of the time efficient calcium phosphate coating on electrospun poly (d, l-lactide). Journal of Biomedical Materials Research Part A, 103(8): 2720-2730.

Mateus DM, Vaz MM and Pinho HJ (2012). Fragmented limestone wastes as a constructed wetland substrate for phosphorus removal. Ecological Engineering, 41: 65-69.

Meng M, Feng Y, Zhang M, Liu Y, Ji Y, Wang J and Yan Y (2013). Highly efficient adsorption of salicylic acid from aqueous solution by wollastonite-based imprinted adsorbent: A fixed-bed column study. Chemical Engineering Journal, 225: 331-339.

Nguyen TAH, Ngo HH, Guo WS, Pham TQ, Li FM, Nguyen TV, and Bui XT (2015). Adsorption of phosphate from aqueous solutions and sewage using zirconium loaded okara (ZLO): fixed-bed

column study. Science of the Total Environment, 523: 40-49.

Price RM, Savabi MR, Jolicoeur JL, and Roy S (2010). Adsorption and desorption of phosphate on limestone in experiments simulating seawater intrusion. Applied Geochemistry, 25(7): 1085-1091.

Sdiri A, Higashi T, Hatta T, Jamoussi F and Tase N (2010). Mineralogical and spectroscopic characterization, and potential environmental use of limestone from the Abiod formation, Tunisia. Environmental Earth Sciences, 61(6): 1275-1287.

Shanmugaprakash M, Sivakumar V, Manimaran M and Aravind J (2014). Batch and dynamics modeling of the biosorption of Cr (VI) from aqueous solutions by solid biomass waste from the biodiesel production. Environmental Progress and Sustainable Energy, 33(2): 342-352.

Sheshdeh RK, Nikou MRK, Badii K, Limaee NY and Golkarnarenji G (2014). Equilibrium and kinetics studies for the adsorption of Basic Red 46 on nickel oxide nanoparticles-modified diatomite in aqueous solutions. Journal of the Taiwan Institute of Chemical Engineers, 45(4): 1792-1802.

Tefera DT, Hashisho Z, Philips JH, Anderson JE and Nichols M (2014). Modeling competitive adsorption of mixtures of volatile organic compounds in a fixed-bed of beaded activated carbon. Environmental science and technology, 48(9): 5108-5117.

Thomas HC (1944). Heterogeneous ion exchange in a flowing system. Journal of the American Chemical Society, 66(10): 1664-1666.

Van Oers CJ, Góra-Marek K, Sadowska K, Mertens M, Meynen V, Datka J and Cool P (2014). In situ IR spectroscopic study to reveal the impact of the synthesis conditions of zeolite β nanoparticles on the acidic properties of the resulting zeolite. Chemical Engineering Journal, 237: 372-379.

Woumfo ED, Siéwé JM and Njopwouo D (2015). A fixed-bed column for phosphate removal from aqueous solutions using an andosol-bagasse mixture. Journal of environmental management, 151: 450-460.

Yang X, Shi Z and Liu L (2015). Adsorption of Sb (III) from aqueous solution by QFGO particles in batch and fixed-bed systems. Chemical Engineering Journal, 260: 444-453.

Yoon YH and NELSON JH (1984). Application of gas adsorption kinetics I. A theoretical model for respirator cartridge service life. The American Industrial Hygiene Association Journal, 45(8): 509-516.

Zeng L, Li X and Liu J (2004). Adsorptive removal of phosphate from aqueous solutions using iron oxide tailings. Water Research, 38(5): 1318-1326.